



JOINT INSTITUTE FOR NUCLEAR RESEARCH  
Flerov Laboratory of Nuclear Reactions

## FINAL REPORT ON THE INTEREST PROGRAMME

*Optimization of the solid ISOL method for  
volatile reaction products of heavy ion  
beam reactions*

**Supervisor:**

Mr. Vedeneev Vyacheslav  
Yurievich, Dubna, Russia

**Student:**

Priyanka Verma, Chandigarh,  
India  
Department of Physics,  
Panjab University

**Participation period:**

(14 February - 25 March)  
Wave 6

## ABSTRACT

In the experiments on synthesis of superheavy nuclei the basic nuclide identification methods are radiochemistry and the ones based on the properties of the decay chains ended by well-known nuclei. Since the half-lives of the majority of superheavy nuclei are quite small (from 100  $\mu$ s till 10 ms), the kinematic separators are widely used for the synthesis of superheavy nuclei, allowing to separate them with a high reliability and efficiency, but they do not measure the masses of nuclei. The mass-spectrometer MASHA was developed at FLNR JINR (Dubna, Russia) to measure the masses of superheavy nuclei and to investigate their  $\alpha$ -decays or spontaneous fission. The MASHA set-up is a combination of the ISOL method of synthesis and separation of radioactive nuclei with the classical method of mass analysis, allowing the mass identification of the synthesized nuclides in a wide mass range.

## 1. INTRODUCTION

The synthesis of new nuclides has stimulated the development of methods for identifying them using the classical mass spectrometric techniques. However, by contrast to the classical mass spectrometry, the masses of new nuclides must be measured online, i.e., directly in the course of their synthesis on accelerated heavy ion beams similarly to the well-known ISOL method. To do this, the Mass Analyzer of Super Heavy Atoms (MASHA) has been designed and produced by the FLNR, JINR. The unique potential of the mass analyzer can be attributed to its capabilities of measuring the masses of synthesized superheavy element isotopes and, simultaneously, of detecting their  $\alpha$  decays and (or) spontaneous fission.

## 2. LAYOUT OF THE SETUP AND ITS KEY PARAMETERS

The setup, the layout of which is shown in Fig. A, consists of the target assembly with a hot catcher; an ion source based on the electron cyclotron resonance (ECR); a magneto-optical analyzer (a mass spectrometer) composed of four dipole magnets (D1, D2, D3a, and D3b), three quadrupole lenses (Q1–Q3), and two sextupole lenses (S1, S2); and a detection system located in the focal plane of the spectrometer.

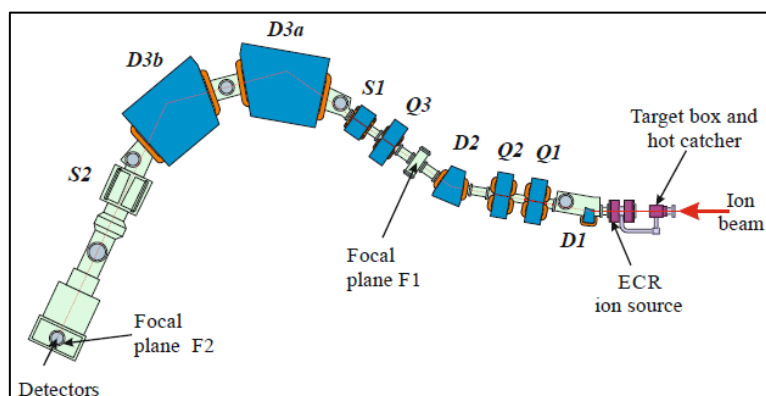


**Fig. A.** Schematic diagram of the MASHA mass separator: (D1, D2, D3a, D3b) dipole magnets, (Q1, Q2, Q3) quadrupole lenses, and (S1, S2) sextupole lenses. The detection system is in focal plane F of the separator.

### 2.1 Ion Source

An ion source based on the ECR (the ECR source) with a 2.45 GHz frequency of its microwave oscillator has been selected for ionizing atoms of nuclear reaction products. In the ECR, atoms are ionized to charge state  $Q = +1$ , accelerated with the aid of the three-electrode system, and gathered into a beam, which is thereafter separated by the magneto-optical system of the mass spectrometer. The ECR source helps to obtain ion currents consisting of almost 100% of singly ionized atoms, and the ionization efficiency of noble gases is as high as 90%.

## 2.2 A Target Assembly and a Hot Catcher

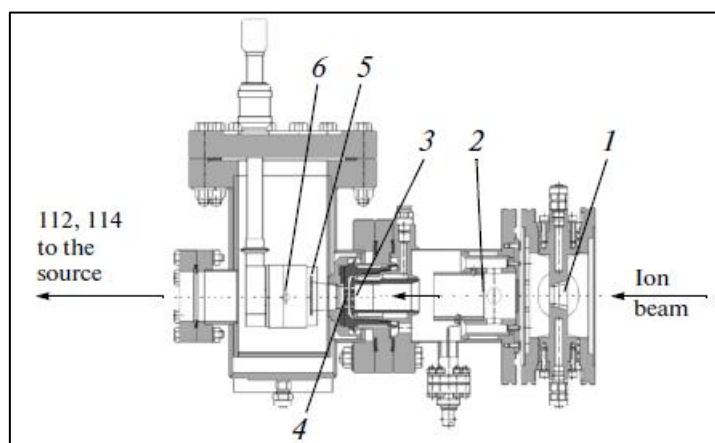


**Fig. B** Target assembly with the hot catcher: (1) split aperture, (2) measuring foil, (3) target, (4) separating foil, (5) graphite absorber, and (6) heater.

A hot catcher was used to inject products of complete fusion reactions into the ECR source. Prior to hitting the target, the primary beam of heavy ions passes through the diagnostic system composed of a split-type aperture of the electrostatic induction sensor. The split aperture is divided into four sectors each of which measures the fraction of the beam current that does not fall into the hole of the aperture. This system allows control of the beam position relative to the ion guide. Physically, the induction sensor is a stainless-steel tube fixed in place on an electrically isolated frame located past the split aperture downstream of the beam and is used to monitor the current in the course of the experiment. Behind the diagnostic system, there was a stationary target (before the upgradations were made in the setup) fixed in place between two grids. Nuclear reaction products escape from the target, pass through the separating foil, and are stopped in the graphite absorber, which is heated to a temperature of 1500–2000 K. In the form of atoms, the products diffuse from the graphite absorber to the vacuum volume of the hot catcher and, moving over the pipeline, reach the ECR source.

## 2.3 Detection and Control System

A special strip detector intended for measuring low direct currents was produced for adjusting the operating modes of the ECR source. It is an exact copy of the frontal part of the silicon detector and looks like a copper multistrip structure on a fiber glass plastic. The pitch of the structure is 1.25 mm, and the total number of strips is 192. When the mass spectrometer was tuned and calibrated, this detector was placed in front of the silicon detector by means of the vacuum-tight feedthrough. A special multichannel electronic module was developed for this detector to measure the low currents. One module is used for 64 channels. The lower threshold or a single channel is 60 pA, and the upper limit is 5  $\mu$ A. The electronic modules are mounted outside the vacuum chamber with the detectors. The data from the modules are transmitted directly to a personal computer via a special interface board.

A well-type silicon detector is installed in the focal plane of the mass spectrometer to detect decays of nuclear reaction products. The plane of the frontal detector part is oriented along the normal to the beam direction. The diagram of the detector with the key dimensions marked in it is shown in Fig. C.

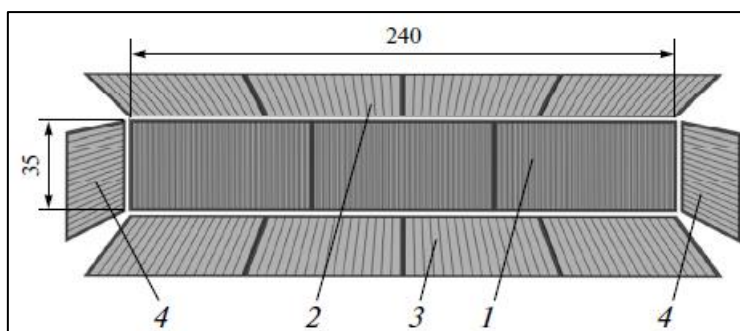


**Fig. C.** Silicon detector of the focal plane: (1) frontal part (192 strips), (2) top part (64 strips), (3) bottom part (64 strips), and (4) side parts (16 strips in each).

The frontal detector part covers a  $240 \times 35$  mm area of the focal plane and consists of 192 strips with a pitch of 1.25 mm. Four side detectors are installed around the frontal detector part to increase the geometrical efficiency of detection of reaction product decays. Each of the top and bottom planes is divided into 64 strips, and each of the left and right planes is divided into 16 strips.

All detector sections are  $300 \mu\text{m}$  thick, and the thickness of the dead layer at the entrance does not exceed 50 nm. The detector assembly in the focal plane is mounted into a single metal frame. The described geometry of the detector assembly makes it possible to detect no less than 90%  $\alpha$  particles emitted in a single nuclear decay at the center of the detector's frontal part. The signals from each strip of the silicon detector are read out independently. The signals arrive at the input of 16-channel charge-sensitive preamplifiers mounted outside the vacuum chamber. The output signals of the preamplifiers are fed to the input of 8-channel shaping amplifiers with an embedded multiplexer.

Two independent data acquisition programs are used in the experiments: one for the silicon detector, and the other for the strip detector measuring low direct currents.

### 3. UPGADATIONS IN MASHA SETUP

The upgrade of some parts of MASHA setup was done during the last years. First of all, target box, ion source, data acquisition system, beam diagnostics and control system were modified.

The modernization of the main units of the mass-spectrometer MASHA was performed. It includes a new design of the hot catcher, the ECR ion source and vacuum chambers, the hot transport system, and installing an additional strip detector at the intermediate plane F1 for the permanent control of the separation efficiency. The design of the hot catcher includes now a poly-graphene heater and a thin catcher made of  $2 \text{ mg/cm}^2$  graphene foil or carbon nanotube paper. This construction has to prevent the catcher from heating and radiation destruction.

The ECR ion source with a special ceramic coating was developed and tested. The possibility to work at a temperature of up to  $300^\circ\text{C}$  and the use of a special chemical inert glass-enamel coating for the inner surfaces of the vacuum pipelines and chambers are the particular features of this design. This is necessary for the MASHA setup to detect not only volatile elements (radon, mercury) but also others close to them (At, Fr, Ac).

### 3.1 Target box

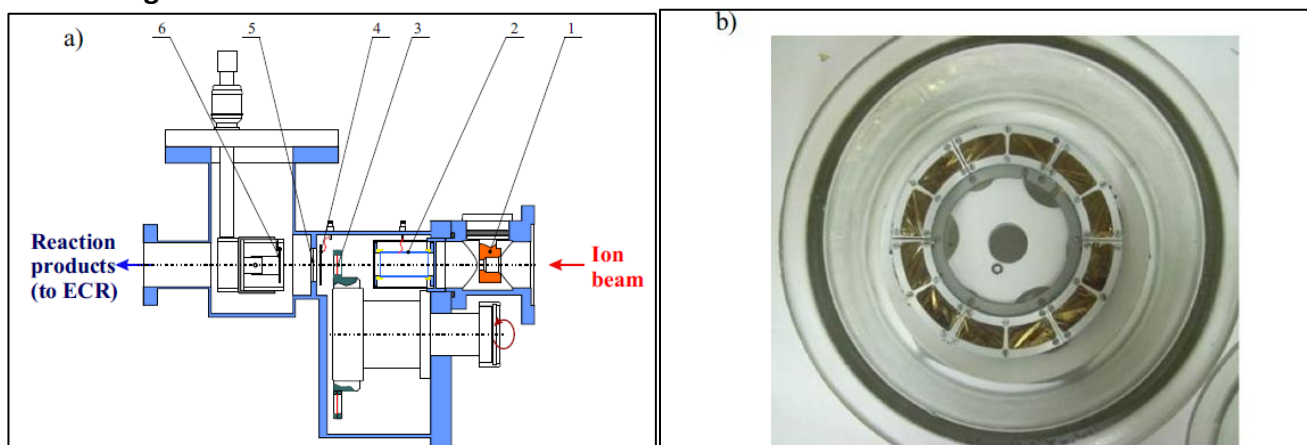


**Fig. I a)** Schematic overview of the target-hot catcher system. Here: 1 – diaphragm; 2 – pick-up sensor; 3 – target on the wheel; 4 – electron emission beam monitor; 5 – separating foil; 6 – hot catcher.

**b)** The photo of the rotating target cassette in assembly. 6 packs, 2 windows at 14 mm width each. Target material –  $^{242}\text{Pu}$  in oxide state put on the Ti 2  $\mu\text{m}$  thick foil.

A schematic overview of the system target + catcher is shown in Fig. I a. This uses the block of rotating targets, assembled into cassettes, which is presented at Fig. I b. The idea to use rotating target instead stationary is better efficiency and heat distribution. Now it's fully modified and represents thermally expanded graphite heated directly by current. This removes the heating losses and irregularity of the heating. The division foil was changed to thin graphite foil in connection to its thermal reliability in comparison to titanium foil.

### 3.2 Ion source

The ion source is operated under ultra-high frequency conditions at about 2.45 GHz. The incoming atoms of nuclear reaction products are ionized to the charge state  $Q = +1$  and accelerated up to 38 keV by a three-electrode electrostatic lens. The ion beam formed is separated by the magneto-optical mass-to-charge ratio analyzer after. Obtained for noble gases, the ionization efficiency is about 90 %. Traditionally the noble gases (krypton, xenon) are chosen for the optimization of the ECR ion source parameters because of its first ionization potentials have maximum values (VIII group of the periodic table) and these are chemical inert elements.

Life time of atoms on the walls depends on the chemical inertia of the wall surface. The walls of the source chamber are covered by titanium nitride (TiN which is chemical inert compound) as well as the walls of catcher and transportation line between. This is made because mercury has a large adhesion on steel and when the atom goes inside the chamber it makes multiple collisions with walls before it ionizes. So, it means that the neutral atom has a very large possibility to “sit” at walls and not to be ionized. That is why a suggestion to cover stainless steel with TiN, which is chemically close to ceramic, was made. Therefore, the ionization efficiency and outgoing time crucially increased. For other elements, such as inert gases the covering affects does not affect or have a minor affect to increase efficiency. The effective using of ion source is to get the most suitable parameters for power, frequency of microwave generator and the pressure of the buffer gas.

### 3.3 Graphite stopper improvement

During the experiments, a detailed study of efficiency and reliability of all systems was also carried out. It turned out that the total separation efficiency of MASHA setup is not stable during the experiments in the case of high beam intensity (up to 10  $\mu\text{A}$  of 48Ca). The high beam intensity corrupts “Hot Catcher” and the separation efficiency of “Hot Catcher” decreases by almost more than five times during a few days.

To prevent this, a little improvement was made which includes an additional foil made of graphene of 0.6  $\text{mg}/\text{cm}^2$

thickness 2.5 mm ahead of main heater at the beam axis. Graphene heats from the main heater by radiation, take some heating load caused by the beam and serves as a separator for low-energy reaction products, which stops inside thin foil, while the beam passes through it and gives almost whole of its energy to graphite heater.

### 3.4 Data acquisition and beam diagnostics

Upgrading, implementation and testing of new DAQ and beam diagnostics using the highspeed digitizers and high-speed digital I/O modules based on PXI and PXIe standards from XIA, Agilent Technologies and National Instruments companies were carried out. The software system for DAQ and beam diagnostics written in C/C++ was also developed and implemented.

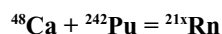
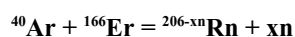
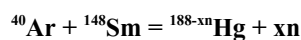
The silicon strip detector (well type) and TIMEPIX were used in the focal plane of mass-separator MASHA. In case of strip detector, the CAMAC DAQ system was replaced by digitizers. Signals from the silicon strips were recorded via independent spectrometric channels.

## 4. THE ISOTOPE SEPARATION ONLINE (ISOL) METHOD

The Isotope Separation OnLine (ISOL) method is widely used in mass analysis for determination of short-lived isotopes. It is based on cooling and stopping the reaction products, making possible their magneto-optic and electrostatic analysis, as well as their separation from the primary beam in the non-interruptible “online” mode. The experiment aimed at studying a new carbon nanomaterials application was performed on the U-400M heavy ion beam at MASHA facility, FLNR, JINR. The main goal of the experiment was to determine the radiation resistance of these materials for the ISOL method. The previous experimental research performed with a thermally expanded graphite heat catcher showed incompatibility with high intensity beams. The improvements made to the ISOL method application allow synthesizing new products at the beam intensities of up to 0.5  $\mu\text{A}$  and higher for the SHE factory perspective.

## 5. Tasks and Results:-

- 1) To perform the analysis of the ISOL (Isotope Separation OnLine) method using experimental data of gathered volatile products for the following reactions:-



- 2) To perform peak analysis of the histograms of counts versus energy for the isotopes of Hg and Rn obtained through above reactions and plot the heatmap for the isotopes and calibrate the energy levels.

## Histograms for Hg isotopes:-

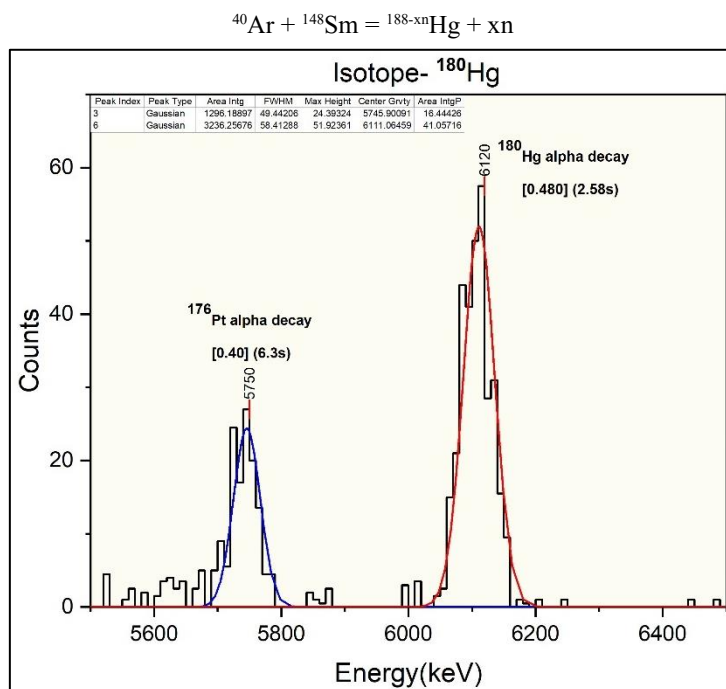


**Figure 1:** Experimental peaks of  $^{180}\text{Hg}$  (6120 keV) &  $^{176}\text{Pt}$  (5750 keV) are identified and the predicted values of alpha decay energies are 6119 keV [99.87] for  $^{180}\text{Hg}$  and 5753 keV [99.74] for  $^{176}\text{Pt}$ .

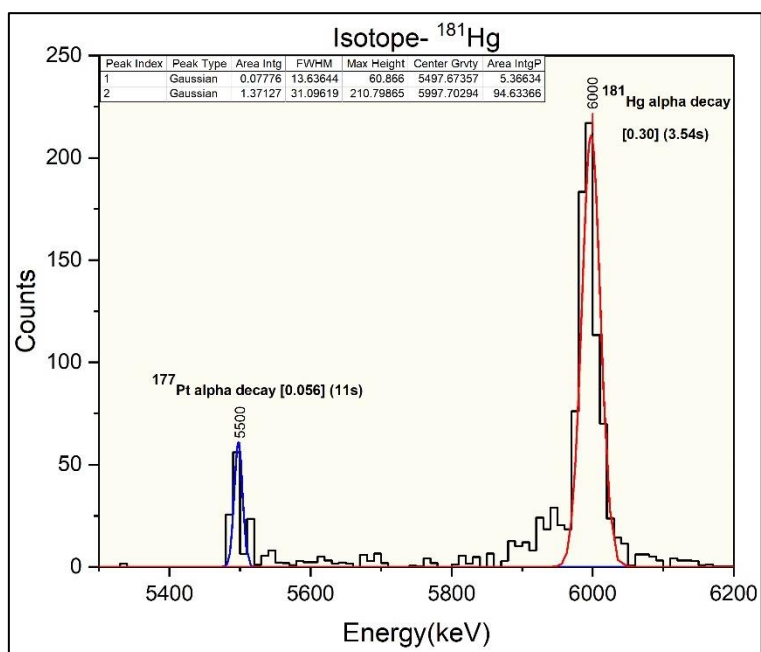


**Figure 2:** Experimental peaks of  $^{181}\text{Hg}$  (6000 keV) &  $^{177}\text{Pt}$  (5500 keV) are identified and the predicted values of alpha decay energies are 6006 keV [87] for  $^{181}\text{Hg}$  and 5517 keV [88.5] for  $^{177}\text{Pt}$ .

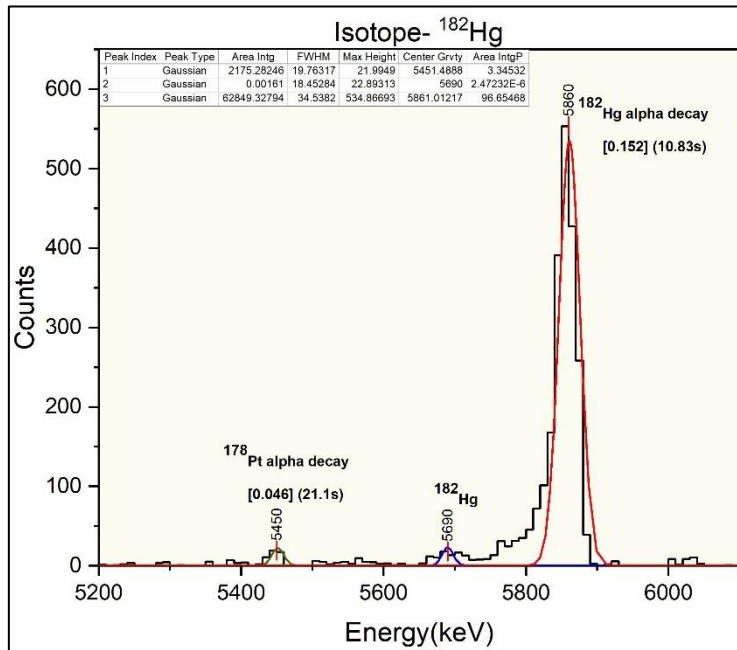


**Figure 3:** Experimental peaks of  $^{182}\text{Hg}$  (5860 keV),  $^{182}\text{Hg}$  (5690 keV) &  $^{178}\text{Pt}$  (5450 keV) are identified and the predicted values of alpha decay energies are 5867 keV [99] and 5700 keV [0.57] for  $^{182}\text{Hg}$  and 5446 keV [94.9] for  $^{178}\text{Pt}$ .

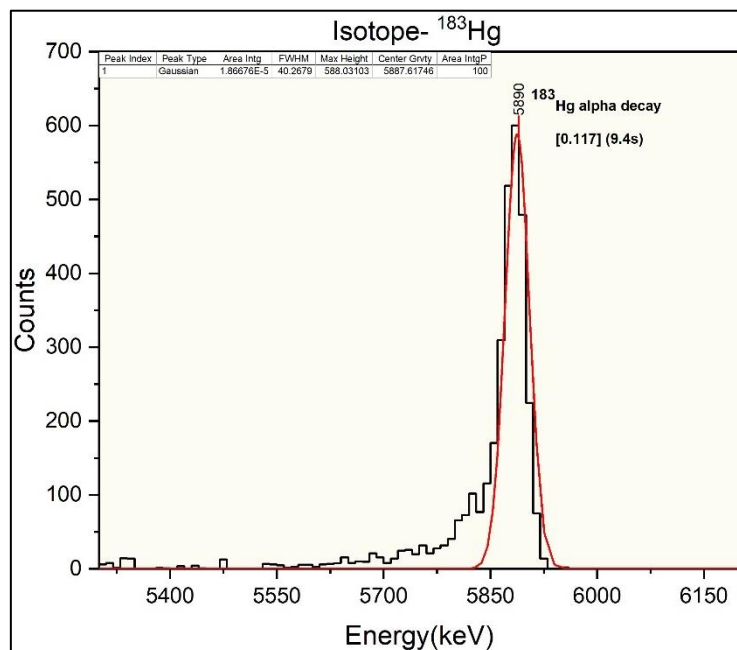


**Figure 4:** Experimental peaks of  $^{183}\text{Hg}$  (5890 keV) is identified but no peak for  $^{179}\text{Pt}$  could be identified and the predicted values of alpha decay energies are 5904 keV [91] for  $^{183}\text{Hg}$  and 5195 keV [100] for  $^{179}\text{Pt}$ .



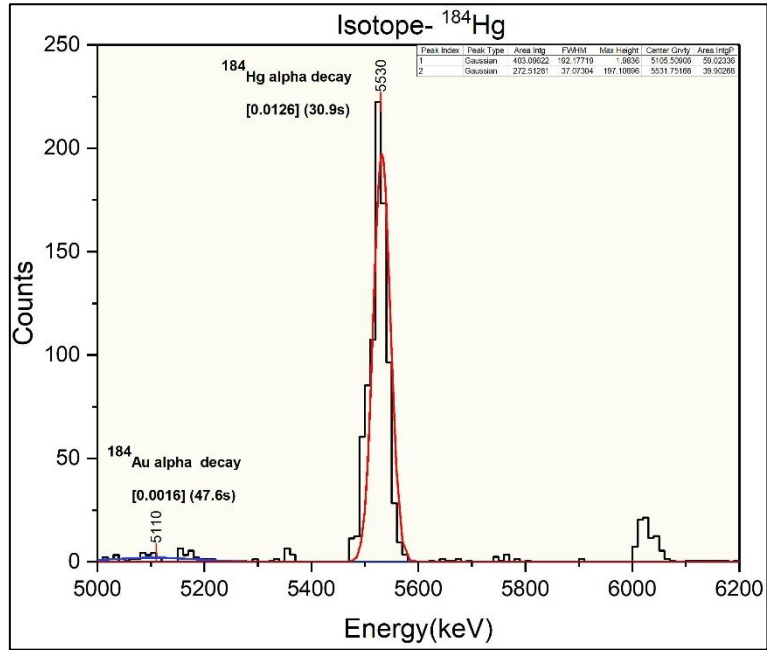


**Figure 5:** Experimental peaks of  $^{184}\text{Hg}$  (5530 keV) and  $^{184}\text{Au}$  (5110 keV) are identified but no peak for  $^{180}\text{Pt}$  could be identified and the predicted values of alpha decay energies are 5535 keV [99.44] for  $^{184}\text{Hg}$  and 5109 keV [46.7] for  $^{184}\text{Au}$  and 5140 keV [92] for  $^{180}\text{Pt}$ .

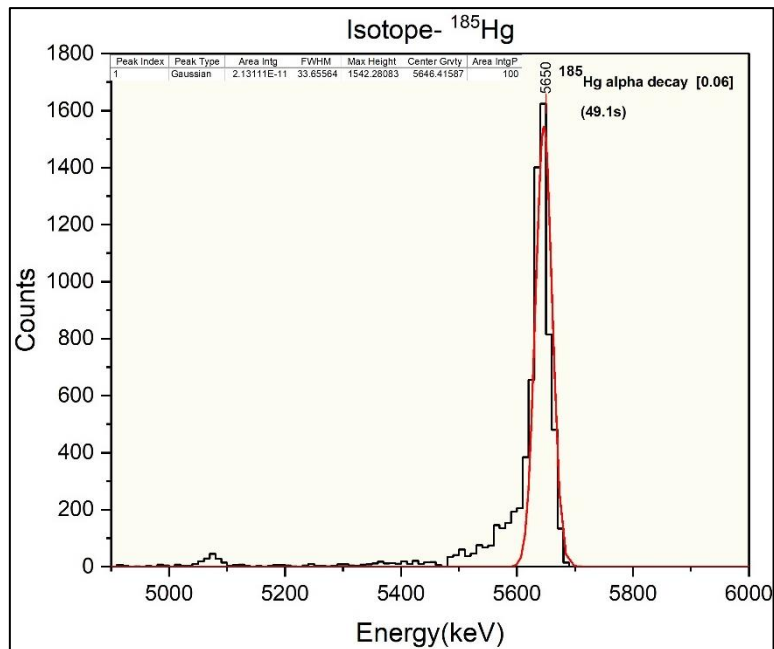


**Figure 6:** Experimental peak of  $^{185}\text{Hg}$  (5650 keV) is identified but no peak could be identified for  $^{181}\text{Pt}$  and the predicted values of alpha decay energies are 5653 keV [96] for  $^{185}\text{Hg}$  and 5036 keV [96.2] for  $^{181}\text{Pt}$ .

**Heat map for mercury isotopes :-**

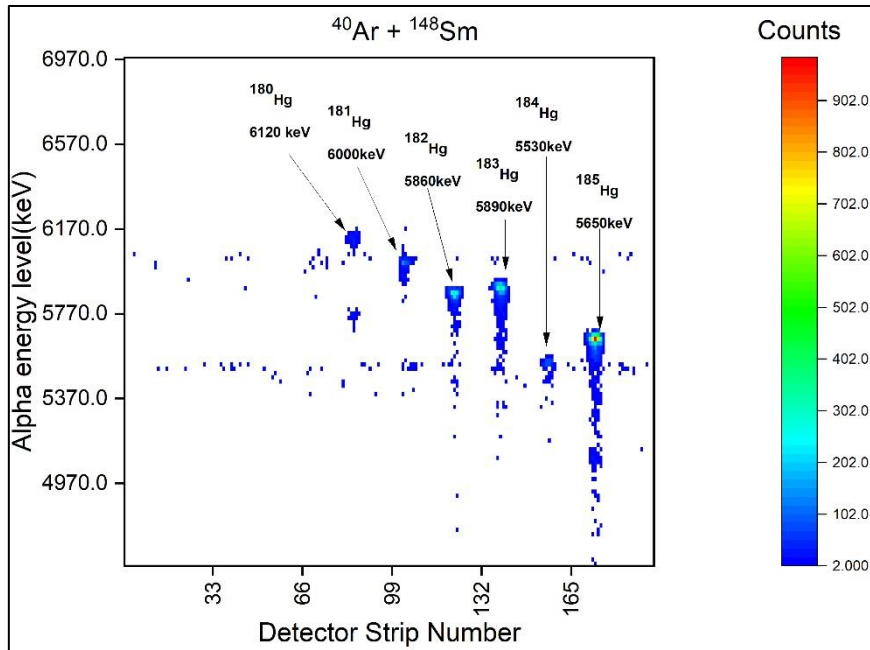


**Figure 7:**  $E_\alpha$  versus Detector strip number for Hg isotopes (A = 180 to 185).

**Histograms for Rn isotopes:-**

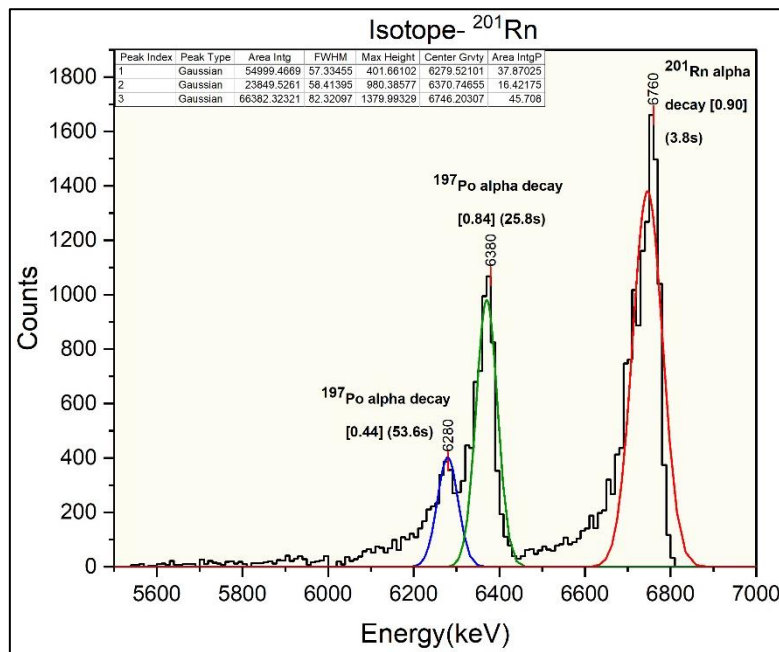
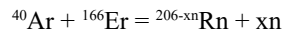


**Figure 8:** Experimental peaks of  $^{201}\text{Rn}$  (6760 keV),  $^{197}\text{Po}$  (6380 keV) and  $^{197}\text{Po}$  (6280 keV) are identified and the predicted values of alpha decay energies are 6773 keV [100] for  $^{201}\text{Rn}$ , 6383.4 keV [99.3] for  $^{197}\text{Po}$  (25.8s) [0.84] and 6281 keV [100] for  $^{197}\text{Po}$  [0.44] (53.6s).

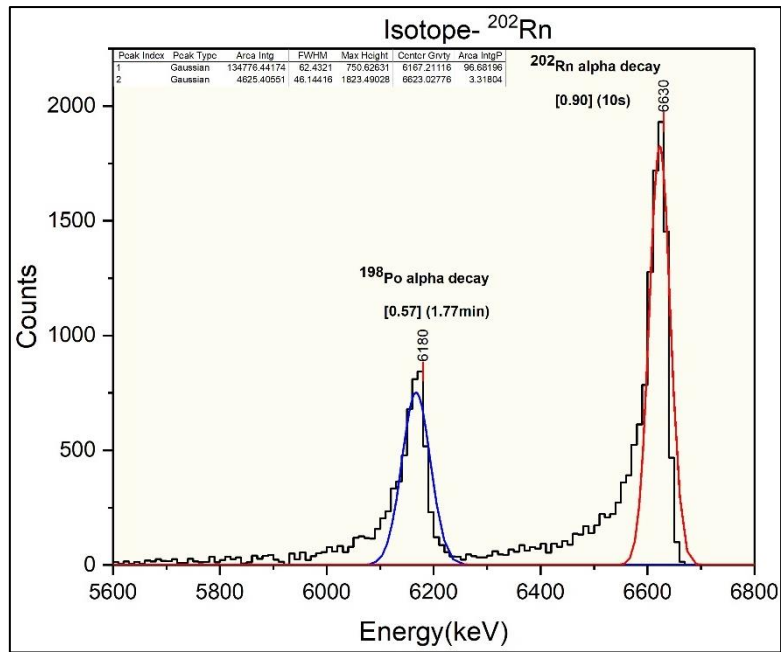


**Figure 9:** Experimental peaks of  $^{202}\text{Rn}$  (6630 keV) &  $^{198}\text{Po}$  (6180 keV) are identified and the predicted values of alpha decay energies are 6639.5 keV [99.9982] for  $^{202}\text{Rn}$  and 6182.0 keV [99.9987] for  $^{198}\text{Po}$ .

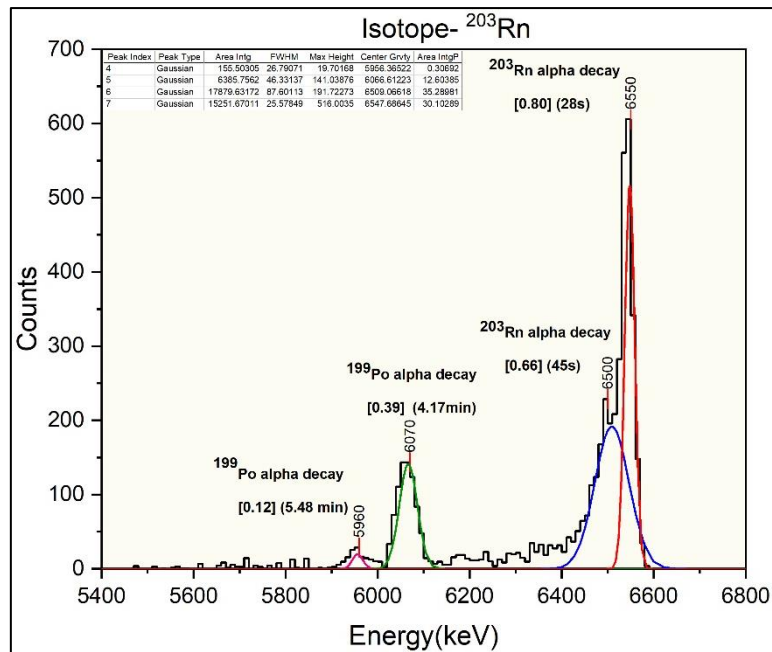


**Figure 10:** Experimental peaks of  $^{203}\text{Rn}$  (6550 keV),  $^{203}\text{Rn}$  (6500 keV),  $^{199}\text{Po}$  (6070 keV) and  $^{199}\text{Po}$  (5960 keV) are identified and the predicted values of alpha decay energies are 6549 keV [100] for  $^{203}\text{Rn}$  [0.80] (28s), 6499.3 keV [97] for  $^{203}\text{Rn}$  [0.66] (45s), 6059 keV [100] for  $^{199}\text{Po}$  [0.39] (4.17 min) and 5952 keV [100] for  $^{199}\text{Po}$  [0.12] (5.48 min).

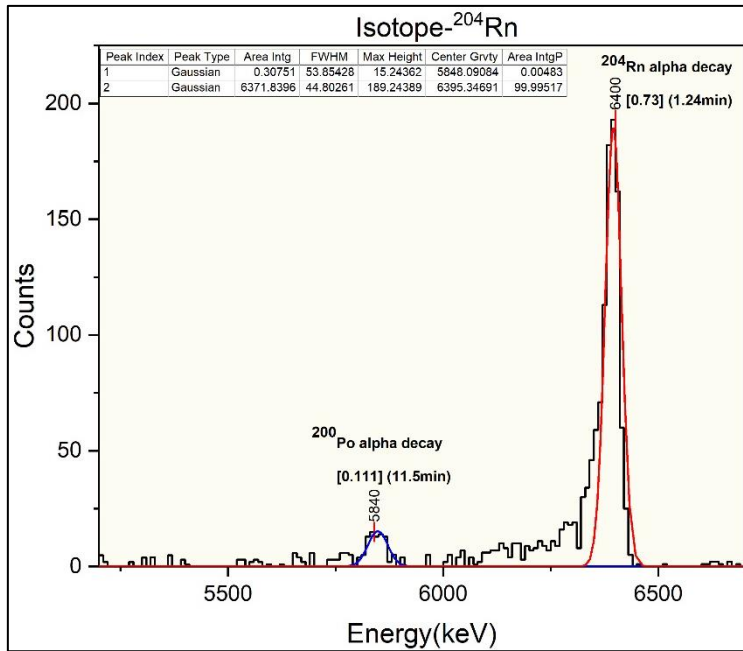


**Figure 11:** Experimental peaks of  $^{204}\text{Rn}$  (6400 keV) &  $^{200}\text{Po}$  (5840 keV) are identified and the predicted values of alpha decay energies are 6418.9 keV for  $^{204}\text{Rn}$  [0.73] and 5861.9 keV [100] for  $^{200}\text{Po}$ .

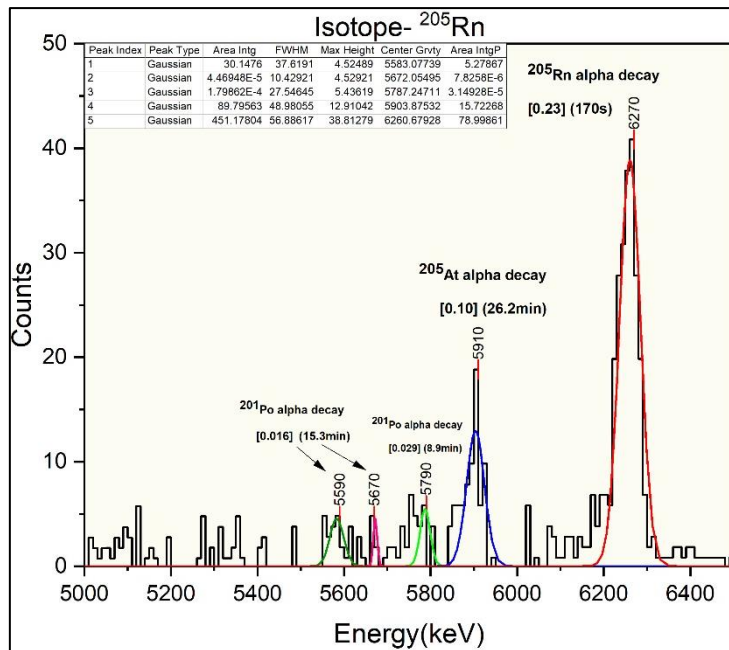


**Figure 12:** Experimental peaks of  $^{205}\text{Rn}$  (6270 keV),  $^{205}\text{At}$  (5910 keV) &  $^{201}\text{Po}$  (5790 keV),  $^{201}\text{Po}$  (5670 keV),  $^{201}\text{Po}$  (5590 keV) are identified and the predicted values of alpha decay energies are 6268 keV [1.8] for  $^{205}\text{Rn}$ , 6262 keV [98.2] for  $^{205}\text{Rn}$ , 5902 keV [100] for  $^{205}\text{At}$  and 5683 keV [98] and 5599 keV [2] for  $^{201}\text{Po}$ .

**Heat map for Rn isotopes:-**

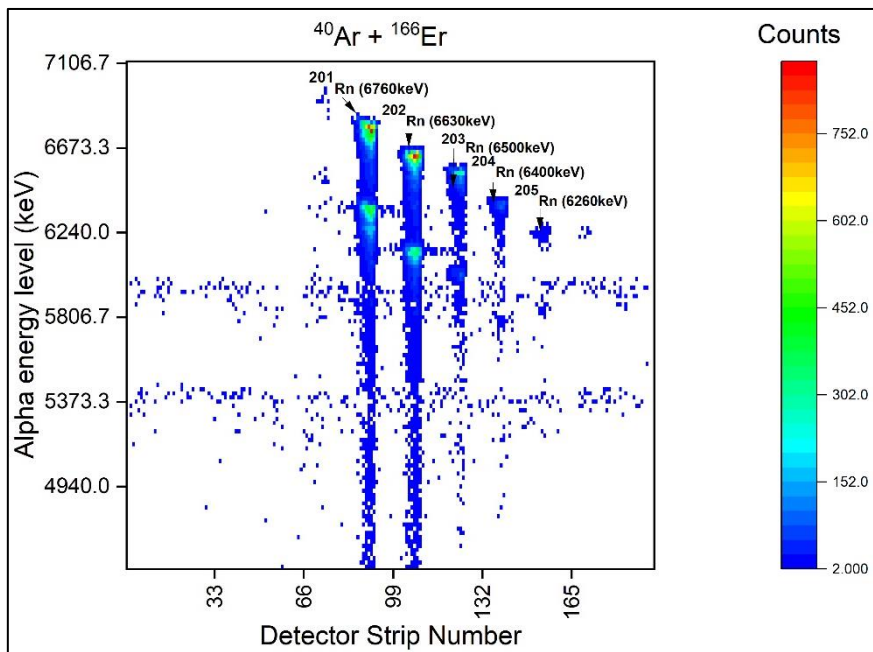


**Figure 13:**  $E_\alpha$  versus Detector strip number for Rn isotopes (A = 201 to 205).

**Histograms for Rn isotopes:-**

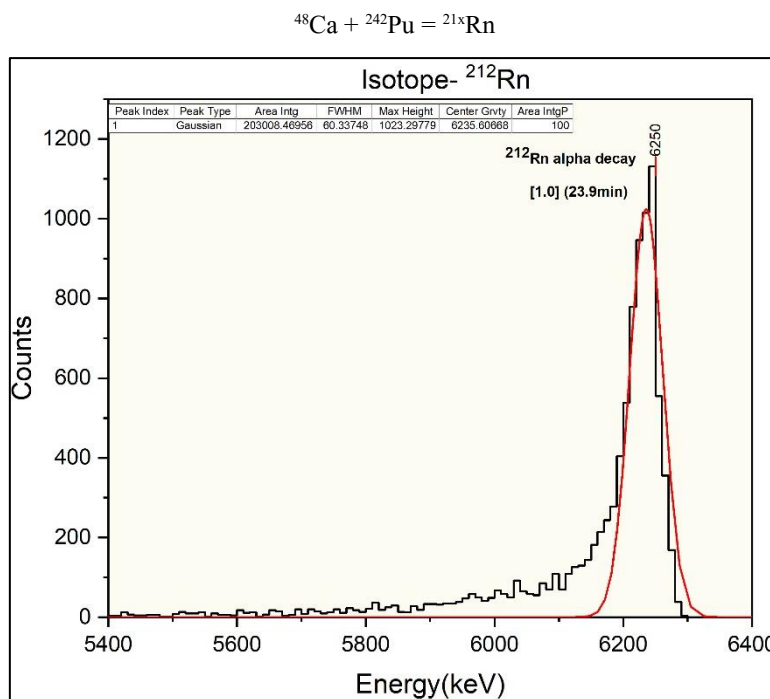


**Figure 14:** Experimental peak of  $^{212}\text{Rn}$  (6250 keV) is obtained but no peak could be identified for  $^{208}\text{Po}$ . The predicted values of alpha decay energies are 6264 keV [99.950] for  $^{212}\text{Rn}$  and 5114.9 keV [99.99976] for  $^{208}\text{Po}$ .

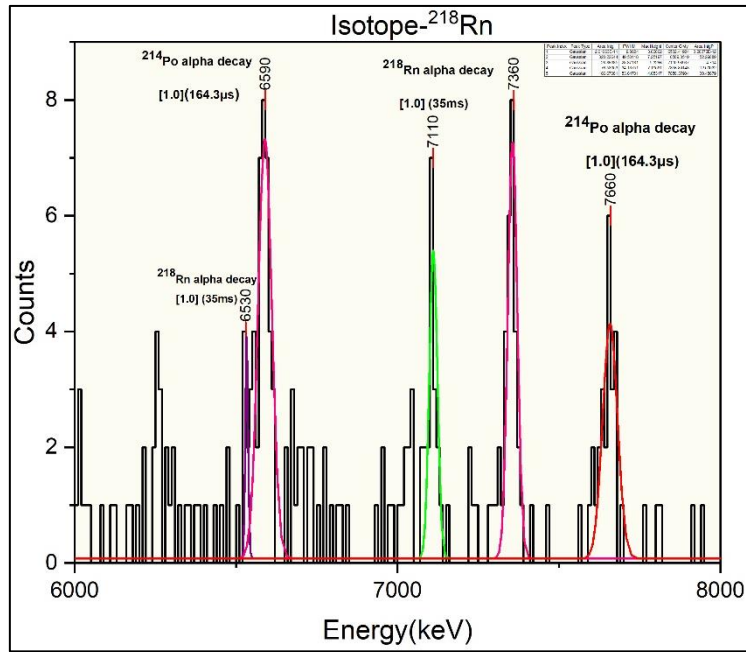


**Figure 15:** Experimental peaks of <sup>218</sup>Rn (6530 keV), <sup>218</sup>Rn (7360 keV), <sup>218</sup>Rn (7110 keV), <sup>214</sup>Po (7660 keV) and <sup>214</sup>Po (6590 keV) are identified and the predicted values of alpha decay energies are 7129.2 keV [99.87] and 6531.2 keV [0.127] for <sup>218</sup>Rn and 7686.82 keV [99.9895] and 6609.8 keV [6E-5] for <sup>214</sup>Po.

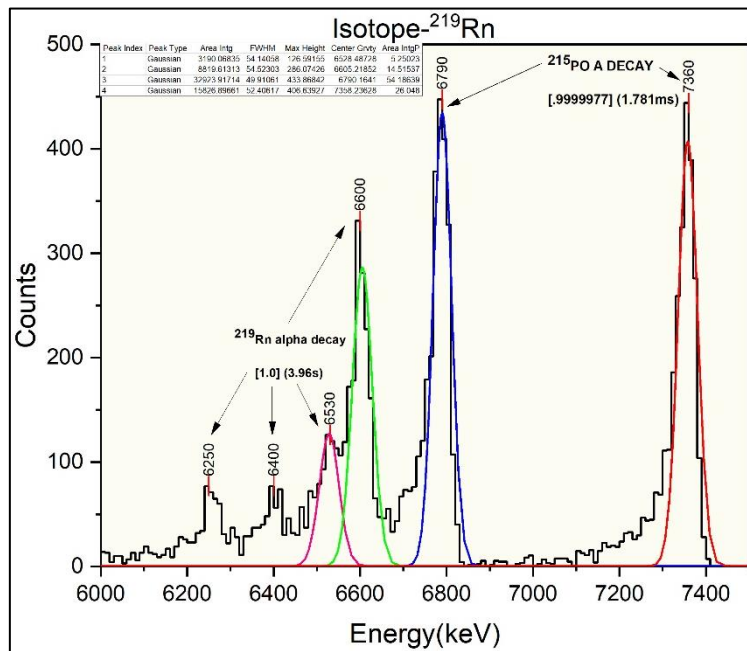


**Figure 16:** Experimental peaks for <sup>219</sup>Rn (6250 keV, 6400 keV, 6530 keV, 6600 keV) and <sup>215</sup>Po (6790 keV, 7360 keV) are identified and the predicted values of alpha decay energies are 6223 keV [0.004], 6425 keV [7.5], 6530 keV [0.12], 6552.6 keV [12.9], 6819.1 keV [79.4] for <sup>219</sup>Rn and 6802 keV [1.6E-3], 7386.1 keV [100] for <sup>215</sup>Po.

## Heat map for Rn isotopes:-

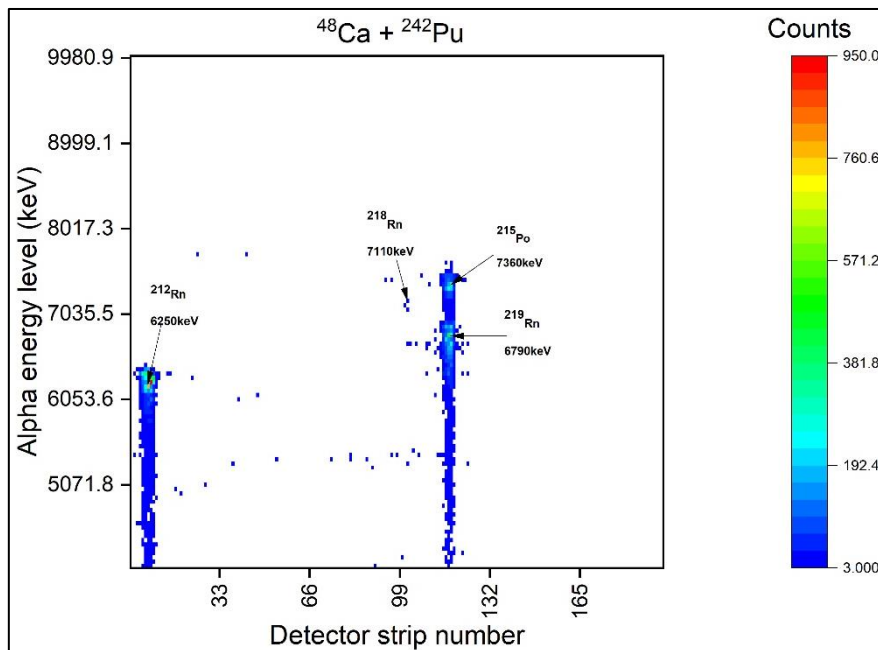


**Figure 17:**  $E_\alpha$  versus detector strip number for Rn isotopes ( $A = 212, 218$  &  $219$ ).

## 6. BENEFITS AND FURTHER PROSPECTS

The upgrade is undertaken in order to increase the total separation efficiency, reduce the separation time, of the installation and working stability and make possible continuous measurements at high beam currents.

In contrast to the old version with the thick carbon catcher now the efficiency of the set-up is almost constant. So, the use of the nanotubes as the hot catcher seems to be very prospective.

The basic results of the performed experiments are:

**a)** It was shown that the separation time did not exceed 1 s. This is two times shorter than in the case of the thick carbon absorber used in old version of the “hot solid-state catcher”.

**b)** the separation efficiency was stable during 85 hours at  $^{40}\text{Ar}$  beam current  $\leq 0,5 \mu\text{A}$ . In the former case the separation efficiency decreased by 6 times during the same period.

Main problem at studying the properties of nuclei close to the stability frontier is the difficulty of their identification. In this aspect applying the TIMEPIX detector system seems to be a very promising.

Another possible application of the mass-separator MASHA would be related to studying the neutron-rich nuclei near the  $N=126$  neutron shell. These nuclei are planned to be produced in the multi-nucleon transfer reactions with mass-to-charge ratio separation of the target-like fragments. The target + catcher system using Isotope Separation On-Line (ISOL), where the target material is solved in the catcher material will be used in this type of reactions. This has to be in favour of increasing the yield of fragments.

It is also expected that a prior determination of masses of the nuclei under investigation will essentially facilitate the analysis of their decays with using the hybrid pixel detectors of the TIMEPIX type. These detectors have a high spatial and energy resolution and allow one to count a single  $\beta$ - or  $\alpha$ -particle. In addition to the  $N = 126$  region one plans also to contribute to investigation of properties of the nuclei near the  $N = 152$  neutron shell. The complete fusion

reactions will be used in this case. These nuclei have been already studied by decay spectroscopy and, in a few cases, by direct mass spectrometry.

## 7. PERSPECTIVES OF USING GAS CATCHER

There are two parameters which are very important for mass-spectrometry: the total separation efficiency and separation time. Since the extraction time of the complex “hot catcher + ECR” is about 1.8–2 seconds, so it allows to register only isotopes with lifetime more or equal this time and, thus, strongly limiting research possibilities. In the past decade gas catchers started to be used widely for production of radioactive beams and turns out to be a perspective way in mass-spectrometry. It has many advantages such as an essentially faster working ( $\tau = 10$  ms instead of  $\tau = 2$  s in graphite solid catcher), no need for an additional ionization, greater efficiency for transformation and matter doesn't suffer from any chemical and physical properties of its own.

## 8. CONCLUSION

The main parts of MASHA setup were described, which are continuously improved. Mercury isotopes were produced in the complete fusion reaction  $^{40}\text{Ar}+^{148}\text{Sm}$  and Rn isotopes are produced via the fusion reaction  $^{40}\text{Ar} + ^{166}\text{Er}$  and from the fusion evaporation reaction of  $^{48}\text{Ca} + ^{242}\text{Pu}$ . The values of alpha decay energies of the isotopes and daughter nuclei, obtained experimentally agreed to the ones predicted theoretically with mild deviations. The peaks of decay energies for certain daughter nuclei could not be obtained owing to their weak intensities or very small lifetimes. After incorporating the upgradations, the experiment showed that the MASHA+TIMEPIX setup could be a powerful instrument for investigation of isotopes far from the stability limits in perspective.

## 9. ACKNOWLEDGEMENT

I am grateful to the people in JINR institute and INTEREST team for organizing this online programme and selecting me for this project. I really appreciate the cooperation while addressing my queries. I would like to extend gratitude towards Mr. Vedeneev Viacheslav Yurievich for being a friendly and supportive project supervisor and for patiently explaining the concepts, solving my queries and providing the necessary information related to the project. My thanks and appreciation also go to my project colleagues who have been supportive throughout this tenure.

## REFERENCES

1. AM Rodin, AV Belozero, DV Vanin, V Yu Vedenev, AV Gulyaev, AV Gulyaeva, SN Dmitriev, MG Itkis, J Kliman, NA Kondratiev, et al. *Masha separator on the heavy ion beam for determining masses and nuclear physical properties of isotopes of heavy and superheavy elements*. Instruments and Experimental Techniques, 57(4):386393, 2014.
2. V Yu Vedenev, AM Rodin, L Krupa, AV Belozero, EV Chernysheva, SN Dmitriev, AV Gulyaev, AV Gulyaeva, D Kamas, J Kliman, et al. *The current status of the masha setup*. Hyperfine Interactions, 238(1):19, 2017.
3. Matthias Schadel and Dawn Shaughnessy. *The chemistry of superheavy elements*. Springer, 2013.
4. AM Rodin, AV Belozero, EV Chernysheva, SN Dmitriev, AV Gulyaev, AV Gulyaeva, MG Itkis, J Kliman, NA Kondratiev, L Krupa, et al. *Separation efficiency of the MASHA facility for short-lived mercury isotopes*. Hyperfine Interactions, 227(1):209221, 2014.
5. *Chemical characterization of element 112*. R. Eichler, N. V. Aksenov, A. V. Belozero et al. Nature. Letters. Vol. 447, May 2007.